JOC The Journal of Organic Chemistry

pubs.acs.org/joc Note

2-λ^5-Phosphaquinolin-2-ones as Non-cytotoxic, Targetable, and pH-Stable Fluorophores

Jeremy P. Bard, Sarah G. Bolton, Holden J. Howard, J. Nolan McNeill, Thaís P. de Faria, Lev N. Zakharov, Darren W. Johnson,* Michael D. Pluth,* and Michael M. Haley*

Cite This: https://doi.org/10.1021/acs.joc.3c01927 Read Online

ACCESS | Metrics & More | Article Recommendations | Supporting Information

ABSTRACT: Several phosphaquinolinone derivatives have been synthesized and characterized to explore their usefulness in the realm of cell imaging. Solution-state photophysical properties in both aqueous and organic solutions were collected for these derivatives. Additionally, CCK-8 cell viability assays and fluorescent imaging in HeLa cells incubated with the new heterocyclic derivatives show evidence of favorable cell permeability, cell viability, and moderate intracellular localization when appended with the well-known morpholine targeting motif.

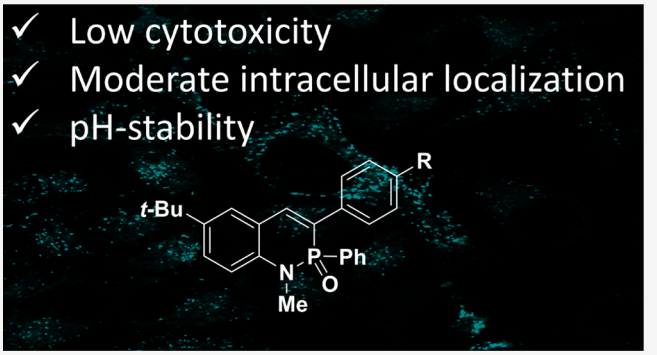

Advancements in cell and tissue imaging have benefited our understanding of biological systems and mechanisms enormously; thus, improvements in new imaging approaches, advanced microscopes, and new functionalizable chromophores remain active areas of chemical biology research. While there has been significant progress in each of these areas, the development of new small molecule chromophores has the potential to not only enable new experimental approaches but also advance the toolbox of available systems that can be coupled with optical outputs.[1−10] One limitation of current fluorophore scaffolds is that although they span different colors and brightnesses, they are derived typically from a relatively small library of "core" molecules, such as coumarins, xanthenes, cyanines, and BODIPY motifs (Figure 1). Prior structure−property relationships for each of these chromophore families have expanded our understanding of how substituents, heteroatom insertion, and backbone modification impact photophysical properties. Modern synthetic chemistry approaches have also broadened the utility of these traditional chromophores to serve as optically responsive fluorescent imaging agents for new biological applications.[11] Conversely, these studies have also revealed some functional limitations such as pH-sensitivity, chemical instability, cytotoxicity, and photobleaching.[12−19] In expanding past these canonical chromogenic platforms, the development of unique chemical structures with modifiable optical properties is critical to further expanding the toolkit of available scaffolds that are compatible with biological imaging.

Recently, we reported that the phosphorus- and nitrogen-containing (PN) scaffold built from a 2-λ^5-phosphaquinolin-2-one framework (Figure 1) possesses interesting photophysical properties, which include coumarin-like fluorescence emission of 450−650 nm, quantum yields up to 93%, structural modularity, and Stokes shifts ranging from 3800−10 000 cm^{-1}.[20,21] In addition to a variety of studies examining the effects of arene core modification[20] and integration of heteroatoms into the scaffold,[22,23] several structure−property relationships have been drawn for substituent group placement on the PN-heterocycle scaffold, which include both the phenyl group on the phosphorus as well as the substituents at the 3- and 6-positions,[24,25] thus guiding the development of the fluorophores in this study (*vide infra*). Moreover, most of the PN-systems are compatible with Lipinski's "Rule of Five", as they have <5 hydrogen bond donors, <10 hydrogen bond acceptors, a mass <500 amu, and a low octanol−water partition coeffient,[26] suggesting that this class of compounds may be cell permeable. Building from these structural parameters, herein we show that this class of PN-heterocycles can function as cell permeable, noncytotoxic, and targetable small molecule fluorophores.

We first examined PN derivative **1** prepared through the cyclization of aniline **2**[21] with $PhP(OPh)_2$ following our standard cyclization procedure (Scheme 1). We chose this initial "test molecule" because of its relatively low molecular

Received: August 25, 2023

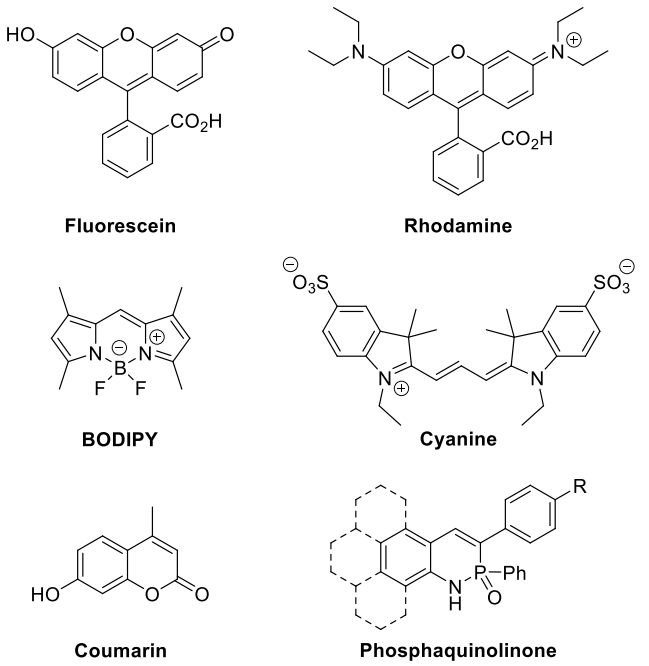

Figure 1. Examples of common fluorophore motifs as well as the phosphaquinolinone scaffold reported here.

Scheme 1. Synthesis of "Test" PN-Heterocycle 1

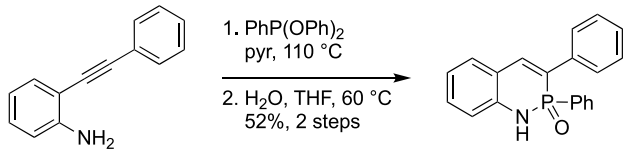

weight, simple molecular structure, and minimal number of H-bond donors and acceptors. To approximate the octanol–water coefficient of **1**, we utilized the SwissADME web tool,[27] which gives a consensus log($P_{o/w}$) value of 3.99.

Examination of the photophysical properties of **1** in $CHCl_3$ (Table 1) revealed two absorbances (Figure 2) at 293 nm (ε = 18 000 M^{-1} cm^{-1}) and 338 nm (ε = 11 000 M^{-1} cm^{-1}), with a corresponding emission (Figure 3) at 441 nm (Φ = 44%, τ = 3.7 ns). These values are in line with our previously reported P–Ph heterocycles, showing a moderate quantum yield likely due to the structural rigidification caused by attaching the phenyl group to the phosphorus center instead of our more traditional phenoxy group.[25] Repeating these experiments in pH 7.4 PBS buffer containing 5% DMSO (Table 1) showed that these photophysical properties were maintained in an aqueous environment. In this more polar solvent system, the absorbances of **1** (Figure 2) shift to slightly higher energy at 290 nm (ε = 17 500 M^{-1} cm^{-1}) and 336 nm (ε = 9140 M^{-1} cm^{-1}), with a small bathochromic shift in emission (Figure 3) to 452 nm (Φ = 23%, τ = 3.6 ns), which were expected changes because of the more polar solvent mixture interacting with our polar fluorophore.

Having established that the emission of **1** is preserved in water, we then examined whether **1** was cell permeable and could maintain its fluorescence in live cells. For these experiments, we treated HeLa cells with ∼10 μM **1** in a DMSO stock solution (final DMSO concentration of 0.5%) for 30 min and imaged the cells by confocal microscopy using a 405 nm excitation. Relatively weak cytosolic fluorescence was observed, which suggested that the platform was cell permeable; however, the luminescent signal strength was relatively poor (Figure S4), which we attributed to the minimal absorptivity of **1** at the 405 nm excitation wavelength (Table S2).

Encouraged by these preliminary results, we modified the PN-based dye to contain an electron-withdrawing and -donating group in the 3- and 6-position, respectively, which results in bathochromic shifts for the absorption and emission in the PN-fluorophore as established in previous studies.[21,24,25] Additionally, the inclusion of a methylated phosphonamide nitrogen in **3** (Scheme 2) should reduce the pH sensitivity and limit self-dimerization through hydrogen bonding. The predicted log ($P_{o/w}$) value of **3** also remains fairly low, with a consensus value of 5.63.[27] Known aniline **4**[28] was protodesilylated with K_2CO_3 and the resultant terminal alkyne underwent Sonogashira cross-coupling with ethyl 4-bromobenzoate (**5**) to afford ethynylaniline **6**. This product was cyclized with $PhP(OPh)_2$ and then hydrolyzed to give heterocycle **7** in a good yield. Next, **7** was treated with MeI and DBU to afford fluorophore **3** in a near quantitative yield after only minimal aqueous washing.

As expected, the photophysical properties of **3** in $CHCl_3$ (Table 1) were more red-shifted than those of **1**, with corresponding absorbance maxima (Figure 2) at 307 nm (ε = 16 200 M^{-1} cm^{-1}) and 369 nm (ε = 7520 M^{-1} cm^{-1}), and an associated emission maximum (Figure 3) at 487 nm (Φ = 24%, τ = 6.1 ns), which shows a slightly lower quantum yield and a longer lifetime potentially due to the greater polarization of the fluorophore in its excited state. Similar shifts were observed in 5% DMSO in PBS (Table 1), with absorbances (Figure 2) at 313 nm (ε = 17500 M^{-1} cm^{-1}) and 382 nm (ε = 10 100 M^{-1} cm^{-1}) and a corresponding emission (Figure 3) at 499 nm (Φ

Table 1. Photophysical Properties of Dyes 1, 3, and 8 at 298 K

compd	$\lambda_{abs,max}$ (nm)	λ_{abs} (nm)	$\varepsilon_{abs,max}$ (M^{-1} cm^{-1})	ε_{abs}[c] (M^{-1} cm^{-1})	λ_{em} (nm)	Stokes shift (nm/cm^{-1})	Φ[d] (%)	$\Phi \times \varepsilon$[e] (M^{-1} cm^{-1})	T[f] (ns)
1 ($CHCl_3$)[a]	293	338	18 000	11 000	441	103/6910	44	7900	3.7
1 (DMSO/PBS)[b]	290	336	17 500	9140	452	116/7638	23	4000	3.6
3 ($CHCl_3$)[a]	307	369	16 200	7520	487	118/6570	24	3900	6.1
3 (DMSO/PBS)[b]	313	382	17 500	10 100	499	117/6140	17	3000	5.9
8 ($CHCl_3$)[a]	306	367	16 700	7500	486	119/6670	63	10 500	5.9
8 (DMSO/PBS)[b]	304	359	21 000	9200	500	141/7855	50	10 500	6.2

[a]All values collected in $CHCl_3$ with ca. 10^{-5} M solutions. [b]All values collected in approximately 5% DMSO in pH 7.4 PBS buffer with ca. 10^{-5} M solutions. [c]Lowest energy absorbance maximum. [d]Calculated with a quinine sulfate standard in 0.1 M H_2SO_4 solution. [e]Brightness value calculated using the lowest energy absorbance maximum. [f]Decay curves were fit to a monoexponential model.

https://doi.org/10.1021/acs.joc.3c01927
J. Org. Chem. XXXX, XXX, XXX–XXX

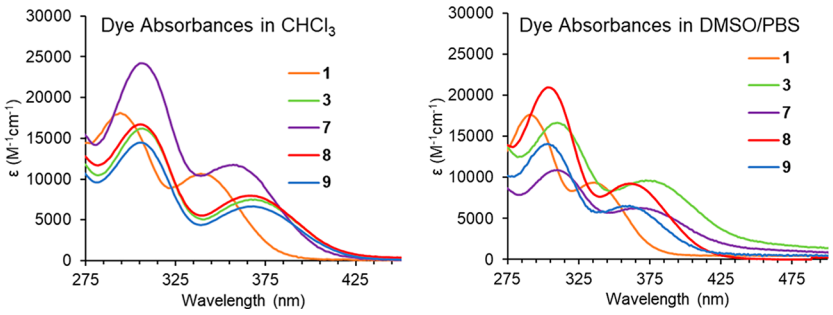

Figure 2. UV−vis absorption spectra of new heterocycles in (left) $CHCl_3$ and (right) ∼5% DMSO in pH 7.4 PBS buffer.

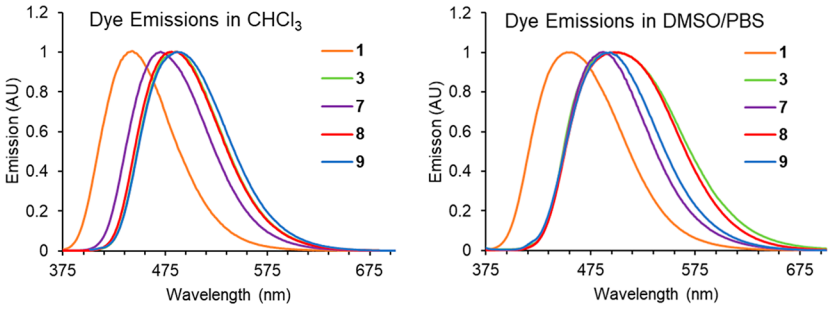

Figure 3. Emission spectra of new heterocycles in (left) $CHCl_3$ and (right) ∼5% DMSO in pH 7.4 PBS buffer.

Scheme 2. Synthesis of Methylated PN-Heterocycle 3 and Morpholine-Containing PN 8

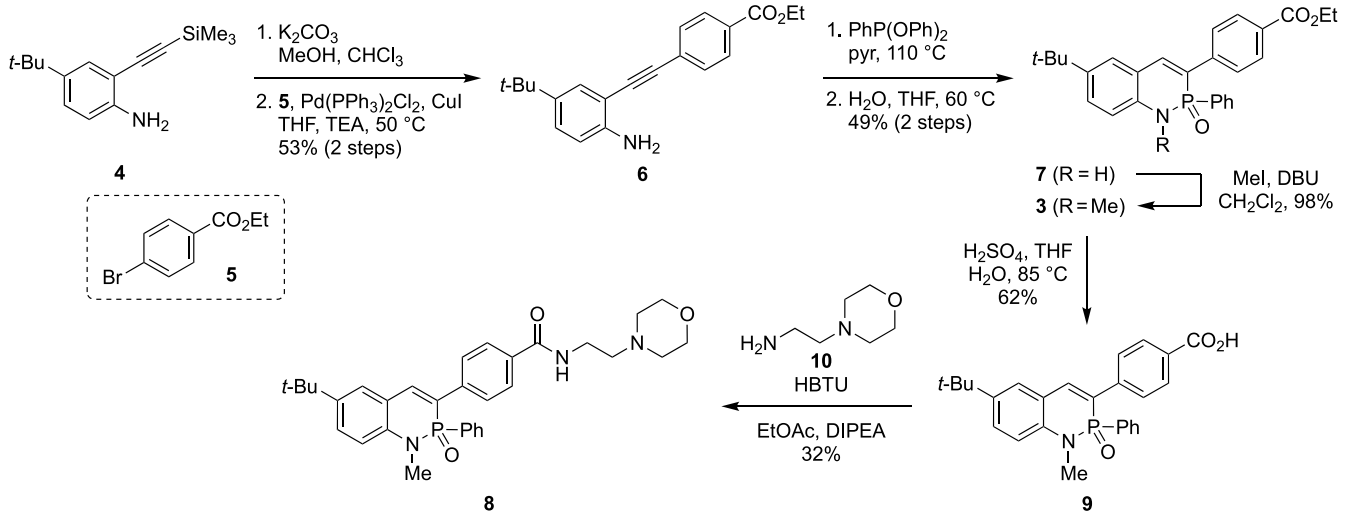

= 17%, τ = 5.9 ns). Highlighting the increased compatibility with 405 nm excitation, the absorption spectrum of **3** has a much higher ε_{405} = 7190 M^{-1} cm^{-1} when compared to the ε_{405} = 183 M^{-1} cm^{-1} of **1** (Table S2), owing to the lower energy absorption peaks being broad enough to still allow for absorbance at 405 nm. Consistent with this increased brightness, we observed a dose-dependent increase in cellular fluorescence for cells treated with 1 to 5 μM **3** (Figure 4a−c). We also investigated the cytotoxicity of **3** in HeLa cells using the CCK-8 cell viability assay after incubation with **3** for 30 min. These experiments showed negligible cytotoxicity up to 150 μM, well above the range of concentrations typically used for cellular imaging (Figure 4d).

To determine whether the PN-scaffold was compatible with subcellular targeting approaches, we prepared heterocycle **8** (Scheme 2) that integrates a lysosome-targeting morpholine unit and a consensus $\log(P_{o/w})$ value of 4.75.[27,29] Ester hydrolysis of **3** gave the intermediate carboxylic acid **9**, which then underwent peptide coupling with HBTU and morpholine derivative **10**[30] to afford **8** in modest yield. Slow diffusion of pentane into a concentrated solution of **8** in $CHCl_3$ gave single crystals suitable for X-ray diffraction. In the resultant structure (Figure S1), the P−N, P═O, P−C, and C−C bond distances are 1.674(3), 1.478(3), 1.784(3), and 1.341(5) Å, respectively, all of which are in line with previously reported parameters.[20] Without the traditional phosphonamide N−H group, however, the molecule forms a 1D hydrogen-bonded "polymer" between the phosphonamide P═O of one molecule and the amide group of its nearest neighbor (Figure S2), with a N···O intermolecular distance of 2.832(4) Å.

The photophysical properties of **8** (Table 1) are nearly identical to those of heterocycle **3** in $CHCl_3$ with absorbances

https://doi.org/10.1021/acs.joc.3c01927
J. Org. Chem. XXXX, XXX, XXX−XXX

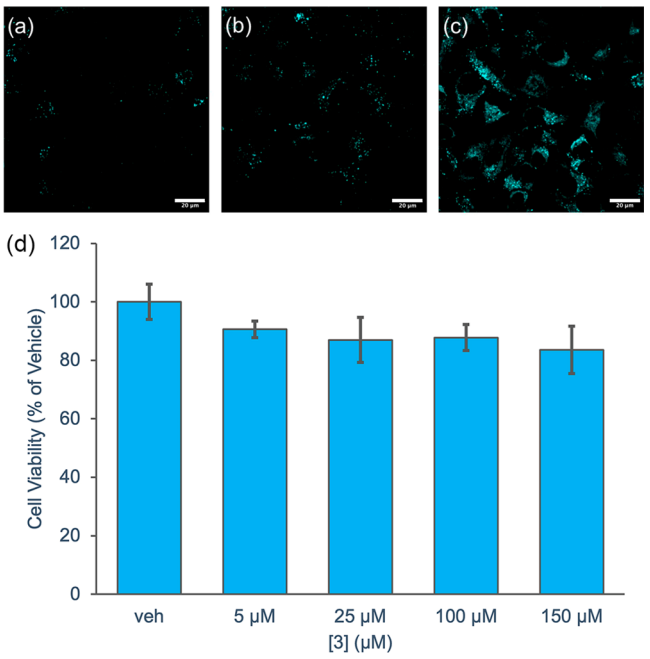

Figure 4. Confocal images of **3** in HeLa cells at (a) 1 μM, (b) 3 μM, and (c) 5 μM after 30 min incubation; scale bar = 20 μm. (d) Cytotoxicity data of **3** in HeLa cells after incubation for 30 min.

(Figure 2) of 306 nm (ε = 16 700 M^{-1} cm^{-1}) and 367 nm (ε = 7500 M^{-1} cm^{-1}) and emission (Figure 3) at 486 nm (Φ = 63%, τ = 5.9 ns). The key difference is the significant increase in the quantum yield of **8**. In 5% DMSO in PBS, however, the lowest energy absorbance (Table 1, Figure 2) is blue-shifted slightly to 359 nm. Consequently, this leads to a moderate decrease in absorption at 405 nm (ε_{405} = 2300 M^{-1} cm^{-1}). The more polar solvent environment, however, does provide a much larger Stokes shift of 141 nm (7855 cm^{-1}) in **8**, with an associated emission (Figure 3) at 500 nm (Φ = 50%).

We also investigated the impacts of methylation on the acid and base sensitivity of **8** in both aqueous and organic solutions. For the aqueous trials, we prepared an ~10 μM solution of **8** in 5% DMSO in deionized H_2O and then adjusted the pH of the solution to 10 or 2 by addition of NaOH or HCl solutions, respectively. Absorption and emission spectra were collected for the initial solutions, immediately following the pH modification, and 18 h later (Figure 5). As expected, the basic conditions led to a negligible change in the spectra of **8**, even after 18 h since the acidic phophonamidate hydrogen is no longer present (Figure 5a). Interestingly, the addition of the acid led to a moderate decrease in the emission of **8** immediately upon the addition of the HCl, which then did not change significantly after 18 h in the solution (Figure 5b). While this decrease is not ideal, the emission remains strong and the molecule appears to remain intact for the duration of the experiment, even in the strongly acidic solution, indicating that this may not hinder potential imaging capabilities.

Repeating a similar study in organic solvents, we made an ~10 μM solution of **8** in $CHCl_3$ and then used it to prepare solutions of **8** in 5% v/v 1,8-diazabicyclo[5.4.0]undec-7-ene (DBU) in $CHCl_3$ and 5% v/v and trifluoroacetic acid (TFA) in $CHCl_3$. Like the aqueous trials, the emission of **8** in the basic solution remains relatively unchanged, but decreases under acidic conditions (Figure S3). While this drop in emission is more substantial in the organic solution, the aqueous solutions

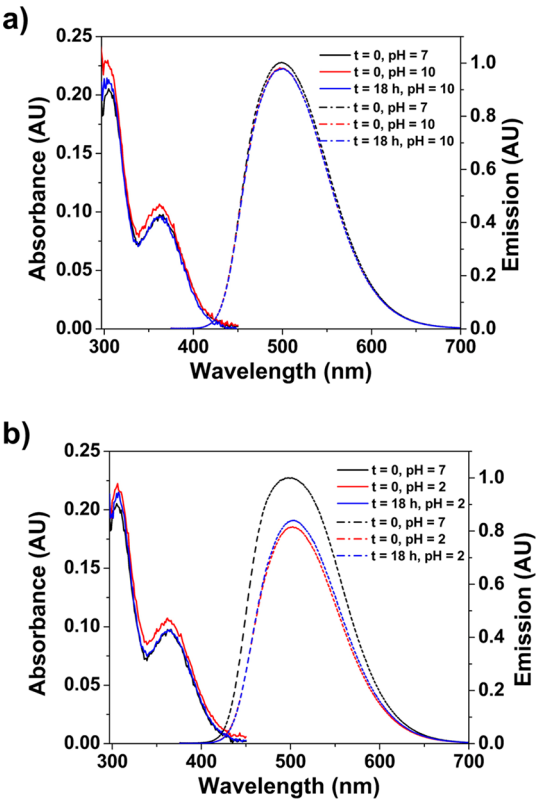

Figure 5. Absorption (solid) and emission (dashed) of **8** in ca. 5% DMSO in H_2O before and after the addition of (a) NaOH to adjust the solution to pH 10 and (b) HCl to adjust to pH 2.

of biological imaging experiments will not see this large drop, and the emission of **8** should still be strong enough to afford good images.

We next tested whether morpholine functionalized **8** was localized to a specific subcellular organelle by comparing its emission in HeLa cells with that of LysoTracker Deep Red. HeLa cells were first incubated with **8** or LysoTracker separately to confirm that there was no spectral bleed through from the different channels. We then coincubated **8** (1 μM, 3 μM, or 5 μM) with 50 nM LysoTracker and measured the colocalization fidelity using the Pearson correlation coefficient (Figures S5–S9). These experiments show moderate colocalization at each concentration with Pearson coefficients of 0.49, 0.61, and 0.65 for the three increasing concentrations, respectively.[31]

In summary, we prepared a small series of fluorescent PN-heterocycles based on the coumarin-like phosphaquinolinone scaffold. These scaffolds maintain their fluorescence in aqueous solution and have excellent pH stability. In addition, structural modification can be used to perturb the photophysical properties. We also demonstrate that these scaffolds are cell permeable and can be imaged by fluorescence microscopy in live cells with minimal cytotoxicity. Moreover, the structure of the PN-heterocycles allows for facile ligation to common targeting motifs. Building from these simple naphthalene-like PN scaffolds, future studies will explore larger acene backbone PN derivatives with longer wavelength absorptions and increased absorption coefficients, expanding the palette of small molecule tools available from this platform.

https://doi.org/10.1021/acs.joc.3c01927
J. Org. Chem. XXXX, XXX, XXX−XXX

EXPERIMENTAL SECTION

General. All oxygen- and water-free reactions were performed under a N_2 atmosphere using the Schlenk technique. Column chromatography was performed using silica gel (240−300 mesh), with solvent systems being referenced to the most abundant solvent. NMR spectra were acquired at room temperature on a Varian Inova 500 (^{1}H: 500 MHz, ^{13}C: 126 MHz, ^{31}P: 202 MHz) or a Bruker Avance III HD 500 equipped with a Prodigy multinuclear cryoprobe (^{1}H: 500 MHz, ^{13}C: 126 MHz, ^{31}P: 202 MHz). ^{1}H and ^{13}C NMR chemical shifts (δ) are expressed in ppm relative to residual $CHCl_3$ (^{1}H: 7.26 ppm, ^{13}C: 77.16 ppm) or DMSO (^{1}H: 2.50 ppm, ^{13}C: 39.52 ppm) shifts. ^{31}P NMR shifts are referenced to 85% H_3PO_4 (δ 0 ppm) as an external reference. UV−vis spectra were recorded by using an Agilent Technologies Cary 60 UV−vis spectrophotometer. Fluorescence emission spectra were recorded using a Horiba Jobin Yvon FluoroMax-4 fluorimeter with excitation at 365 nm. Quantum yields (ϕ) were determined through comparison of the emission and absorption intensities of the analyte to those of a 0.1 M H_2SO_4 quinine sulfate solution.[32] Fluorescence lifetime measurements were recorded by using a Horiba FluoroHub Single Photon Counting Controller with a TemPro Fluorescence Lifetime System attachment. Acid- and base-stability studies were performed by using a Tecan Spark 20 M plate reader. High-resolution mass spectra (HRMS) were recorded on a Waters XEVO G2-XS quadrupole time-of-flight (QToF) mass spectrometer. Compounds **2**,[21] **4**,[28] and **10**[31] were prepared as previously described. LysoTracker Deep Red (Thermo Fisher) and CCK-8 (Dojindo) were purchased.

PN-Heterocycle ***1***. A solution of aniline **2** (665 mg, 3.4 mmol, 1 equiv) and $PhP(OPh)_2$ (2.0 g, 6.9 mmol, 2 equiv) in pyridine (4 mL) was stirred in a round-bottom flask at 110 °C (sand bath) for 48 h. After the mixture was cooled to room temperature, toluene (20 mL) was added, and the solvent was removed *in vacuo*. Two more analogous toluene washes were performed to fully remove pyridine from the mixture. The crude residue was dissolved in minimal THF, H_2O (5 drops) was added, and then the solution was stirred to 60 °C (water bath) for 1 h. The mixture was dried (Na_2SO_4), filtered, and concentrated *in vacuo*. Column chromatography (2:1:1 hexanes:EtOAc:CH_2Cl_2, R_f = 0.15) and subsequent recrystallization from CH_2Cl_2 and hexanes gave **1** (565 mg, 52%) as a yellow solid: mp >250 °C; ^{1}H NMR (500 MHz, $CDCl_3$) δ 7.66 (d, J = 7.1 Hz, 1H), 7.65−7.61 (m, 1H), 7.62 (d, J = 32.7 Hz, 1H), 7.61−7.56 (m, 3H), 7.38 (t, J = 8.0 Hz, 2H), 7.33−7.17 (m, 6H), 7.01 (d, J = 8.1 Hz, 1H), 6.99 (t, J = 7.4 Hz, 1H). ^{13}C{^{1}H} NMR (126 MHz, $CDCl_3$) δ 139.6 (d, J = 3.6 Hz), 139.0 (d, J = 4.0 Hz), 136.9 (d, J = 11.5 Hz), 133.2 (d, J = 138.6 Hz), 132.6 (d, J = 10.6 Hz), 132.0 (d, J = 2.8 Hz), 130.6, 130.5, 128.7, 128.3, 128.2, 127.9 (d, J = 5.9 Hz), 127.3 (d, J = 117.7 Hz), 120.8, 119.6 (d, J = 12.3 Hz), 117.2 (d, J = 7.7 Hz). ^{31}P NMR (202 MHz, $CDCl_3$) δ 11.99; HRMS (ASAP) $[M + H]^+$ calcd for $C_{20}H_{17}NOP$ 318.1048, found 318.1032.

Aniline ***6***. Aniline **4** (2.18 g, 8.9 mmol, 1.0 equiv) and K_2CO_3 (3.70 g, 26.7 mmol, 3.0 equiv) in MeOH (35 mL) and $CHCl_3$ (35 mL) were stirred at room temperature for 1.5 h. Once the reaction was complete by TLC, the mixture was reduced *in vacuo*. The crude material was then suspended in CH_2Cl_2 (20 mL) and washed 3× with H_2O. The organic layer was collected, dried (Na_2SO_4), and concentrated *in vacuo*. The crude terminal acetylene was then carried forward to the next step.

Ester **5** (2.04 g, 8.9 mmol, 1.0 equiv), CuI (119 mg, 0.623 mmol, 0.07 equiv), $Pd(PPh_3)_2Cl_2$ (437 mg, 0.623 mmol, 0.07 equiv), and the crude terminal acetylene were dissolved in THF (30 mL), and the solution was made air-free using four rounds of atmosphere exchange with N_2. Et_3N (30 mL) was then added via syringe, and the reaction mixture was stirred to 50 °C (sand bath) for 48 h. After the mixture was cooled to room temperature, it was concentrated *in vacuo*. EtOAc (3 × 20 mL) was added to the reaction mixture and subsequently removed *in vacuo* to remove the residual Et_3N. Column chromatography (16:1:1 hexanes:EtOAc:CH_2Cl_2, R_f = 0.20) afforded aniline **6** (1.53 g, 53%) as an orange solid: mp 97.5−98.8 °C; NMR ^{1}H NMR (500 MHz, $CDCl_3$) δ 8.03 (d, J = 8.4 Hz, 2H), 7.58 (d, J = 8.4 Hz, 2H), 7.39 (d, J = 2.4 Hz, 1H), 7.21 (dd, J = 8.5, 2.3 Hz, 1H), 6.69 (d, J = 8.5 Hz, 1H), 4.39 (q, J = 7.1 Hz, 2H), 4.18 (s, 2H), 1.41 (t, J = 7.2 Hz, 3H), 1.29 (s, 9H). ^{13}C{^{1}H} NMR (126 MHz, $CDCl_3$) δ 166.1, 145.6, 141.0, 131.3, 129.7, 129.5, 128.8, 128.1, 127.7, 114.4, 106.9, 93.6, 89.6, 61.1, 33.9, 31.4, 14.3; HRMS (ASAP) $[M + H]^+$ calcd for $C_{21}H_{24}NO_2$ 322.1807, found 322.1816.

PN-Heterocycle ***7***. A mixture of aniline **6** (960 mg, 2.98 mmol, 1.0 equiv) and $PhP(OPh)_2$ (1.76 g, 5.96 mmol, 2.0 equiv) in pyridine (5 mL) was stirred in a round-bottom flask at 110 °C (sand bath) for 48 h. After the mixture was cooled to room temperature, toluene (20 mL) was added, and the solvent was removed *in vacuo*. Two more analogous toluene washes were performed to fully remove pyridine from the mixture. The crude residue was then dissolved in minimal THF, H_2O (5 drops) was added, and then the solution was heated to 60 °C (water bath) for 1 h. The mixture was then dried (Na_2SO_4), filtered, and concentrated *in vacuo*. Column chromatography (5:1:1 → 1:1:1 hexanes:EtOAc:CH_2Cl_2, R_f = 0.15 in 3:1:1) and subsequent recrystallization from CH_2Cl_2 and hexanes gave heterocycle **7** (652 mg, 49%) as a yellow solid: mp >250 °C; NMR ^{1}H NMR (500 MHz, $CDCl_3$) δ 7.90 (d, J = 8.4 Hz, 2H), 7.77 (d, J = 3.0 Hz, 1H), 7.68 (d, J = 31.1 Hz, 1H), 7.67 (d, J = 8.1 Hz, 2H), 7.63 (d, J = 7.3 Hz, 1H), 7.60 (d, J = 7.3 Hz, 1H), 7.40 (d, J = 2.3 Hz, 1H), 7.38−7.31 (m, 2H), 7.24 (dt, J = 7.5, 3.9 Hz, 2H), 6.99 (d, J = 8.5 Hz, 1H), 4.32 (q, J = 7.1 Hz, 2H), 1.36 (t, J = 7.2 Hz, 3H), 1.34 (s, 9H). ^{13}C{^{1}H} NMR (126 MHz, $CDCl_3$) δ 166.4, 143.6, 141.5 (d, J = 11.6 Hz), 140.9 (d, J = 3.2 Hz), 132.8 (d, J = 139.4 Hz), 132.5 (d, J = 10.8 Hz), 131.9 (d, J = 2.7 Hz), 129.7, 129.4, 128.5, 128.2, 128.1, 127.6 (d, J = 6.2 Hz), 127.1, 126.0 (d, J = 119.1 Hz), 118.7 (d, J = 12.1 Hz), 117.0 (d, J = 7.6 Hz), 61.0, 34.2, 31.4, 14.3. ^{31}P NMR (202 MHz, $CDCl_3$) δ 11.79; HRMS (ASAP) $[M + H]^+$ calcd for $C_{27}H_{29}NO_3P$ 446.1888, found 446.1885.

PN-Heterocycle ***3***. Heterocycle 7 (78 mg, 0.175 mmol, 1.0 equiv) was dissolved in dry CH_2Cl_2 (5 mL), and the mixture was put under N_2 via an atmosphere exchange. MeI (0.9 mL, 3.95 mmol, 22.5 equiv) was added. DBU (0.4 mL, 1.75 mmol, 10 equiv) was then added dropwise, which induced an immediate red-shift in both the absorption and emission color of the solution. The mixture was stirred for 16 h (complete by TLC), at which point the solution returned to its original color. The mixture was then reduced *in vacuo*, before being dissolved in CH_2Cl_2, washed 3× with an aqueous $NaHCO_3$ solution to remove excess DBU. The organic layer was dried (K_2CO_3), filtered, and concentrated *in vacuo* furnish **3** (79 mg, 98% yield) as a yellow solid: mp = 125.4−126.8 °C; NMR ^{1}H NMR (500 MHz, $CDCl_3$) δ 7.91 (d, J = 8.1 Hz, 2H), 7.83−7.61 (m, 5H), 7.50 (d, J = 8.7 Hz, 1H), 7.46 (s, 1H), 7.39 (t, J = 6.7 Hz, 1H), 7.34 (td, J = 7.5, 3.2 Hz, 2H), 7.04 (d, J = 8.7 Hz, 1H), 4.33 (q, J = 7.1 Hz, 2H), 3.12 (d, J = 7.7 Hz, 3H), 1.37 (s, 9H), 1.35 (t, J = 7.0 Hz, 3H). ^{13}C{^{1}H} NMR (126 MHz, $CDCl_3$) δ 166.4, 143.3, 141.4 (d, J = 11.7 Hz), 141.0 (d, J = 3.0 Hz), 139.5, 132.4 (d, J = 10.5 Hz), 132.2 (d, J = 138.1 Hz), 132.0 (d, J = 2.8 Hz), 129.7, 129.5, 128.7, 128.5, 128.4, 127.7 (d, J = 6.2 Hz), 125.7 (d, J = 117.8 Hz), 120.0 (d, J = 11.5 Hz), 112.9 (d, J = 5.0 Hz), 61.0, 34.1, 31.5 (d, J = 4.0 Hz), 31.4, 14.3. ^{31}P NMR (202 MHz, $CDCl_3$) δ 16.75; HRMS (ASAP) $[M + H]^+$ calcd for $C_{28}H_{31}NO_3P$ 460.2042, found 460.2068.

Acid ***9***. To heterocycle **3** (200 mg, 0.435 mmol, 1.0 equiv) in THF (20 mL) was added H_2SO_4 (20 mL, 30% v:v in H_2O). The mixture was stirred at 85 °C (sand bath) under a reflux condenser for 24 h. After cooling to room temperature, the reaction mixture was extracted with EtOAc (5 × 40 mL). The organic layer was dried (K_2CO_3), filtered, and concentrated *in vacuo*. Several rounds of recrystallization from CH_2Cl_2 and pentanes removed residual EtOAc and afforded carboxylic acid **9** (117 mg, 62%) as a yellow solid: mp >250 °C; NMR ^{1}H NMR (500 MHz, DMSO-d_6) δ 8.06 (d, J = 31.2 Hz, 1H), 7.83 (d, J = 8.2 Hz, 2H), 7.79 (d, J = 8.1 Hz, 2H), 7.71 (s, 1H), 7.63−7.52 (m, 3H), 7.49−7.39 (m, 3H), 7.14 (d, J = 8.8 Hz, 1H), 2.99 (d, J = 7.6 Hz, 3H), 1.33 (s, 9H). ^{13}C{^{1}H} NMR (126 MHz, DMSO-d_6) δ 166.9, 142.6, 141.1, 141.0, 139.1, 132.3 (d, J = 134.5 Hz), 132.1, 131.8 (d, J = 10.8 Hz), 129.4, 129.3 (d, J = 105.0 Hz), 128.7, 128.6 (d, J = 8.9 Hz), 127.4 (d, J = 6.1 Hz), 124.9, 123.9, 119.5 (d, J = 11.2 Hz), 113.1, 33.8, 31.2, 31.1. ^{31}P NMR (202 MHz, DMSO-d_6) δ 15.7;

https://doi.org/10.1021/acs.joc.3c01927
J. Org. Chem. XXXX, XXX, XXX−XXX

HRMS (ASAP) $[M + H]^+$ calcd for $C_{26}H_{27}NO_3P$ 432.1729, found 432.1758.

PN-Heterocycle **8**. Acid **9** (314 mg, 0.730 mmol, 1.0 equiv) and HBTU (554 mg, 1.46 mmol, 2.0 equiv) were added to a round-bottom flask, which was then put under an N_2 atmosphere via atmosphere exchange. This mixture was dissolved in dry CH_2Cl_2 (18 mL) before 4-(2-aminoethyl)morpholine (**10**, 0.38 mL, 2.92 mmol, 4.0 equiv) was added. Lastly, DIPEA (0.140 mL, 0.82 mmol, 1.0 equiv) was added via syringe. The reaction was stirred for 1 h at which point TLC showed complete conversion of starting material. The mixture was then concentrated *in vacuo* before being suspended in MeCN and cooled in an ice bath for 1 h. The precipitated salt byproducts were removed by filtration, and the organic solution was then reduced to dryness *in vacuo*. The crude material was redissolved in minimal CH_2Cl_2, pentanes were slow-layered, and the mixture was left overnight. This initial process led to a brown oil coating the bottom of the flask, which allowed for a cleaner product solution to be decanted, reconcentrated, and set up for another round of recrystallization following the same procedure. This afforded a fluorescent, yellow oil suspending on the bottom of the flask with crystalline yellow solids dotted throughout. The organic layer was removed, and the oil/solid mixture was dried *in vacuo* to afford **8** (126 mg, 32% yield) as a yellow solid: mp = 234.5−235.9 °C. ^{1}H NMR (500 MHz, DMSO-d_6) δ 8.35 (t, J = 5.7 Hz, 1H), 8.04 (d, J = 31.4 Hz, 1H), 7.80−7.66 (m, 5H), 7.64−7.51 (m, 3H), 7.48 (td, J = 7.3, 1.5 Hz, 1H), 7.43 (td, J = 7.1, 3.3 Hz, 2H), 7.13 (d, J = 8.7 Hz, 1H), 3.55 (t, J = 4.6 Hz, 4H), 3.35 (d, J = 6.7 Hz, 2H), 2.99 (d, J = 7.6 Hz, 3H), 2.42 (t, J = 7.0 Hz, 2H), 2.39 (t, J = 4.0 Hz, 4H), 1.34 (s, 9H). ^{13}C{^{1}H} NMR (126 MHz, DMSO-d_6) δ 165.6, 142.5, 140.6, 139.2 (d, J = 12.0 Hz), 139.0, 133.5, 132.4 (d, J = 134.8 Hz), 132.05, 132.02, 131.7 (d, J = 10.3 Hz), 128.6 (d, J = 13.1 Hz), 128.4, 127.3, 127.1 (d, J = 6.2 Hz), 124.5 (d, J = 116.9 Hz), 119.5 (d, J = 11.3 Hz), 113.0, 66.2, 57.3, 53.3, 36.5, 33.8, 31.2, 31.0 (d, J = 3.7 Hz). ^{31}P NMR (202 MHz, DMSO-d_6) δ 15.77; HRMS (ASAP) $[M + H]^+$ calcd for $C_{32}H_{39}N_3O_3P$ 544.2729, found 544.2737.

■ ASSOCIATED CONTENT

Data Availability Statement

The data underlying this study are available in the published article and its online Supporting Information.

Supporting Information

The Supporting Information is available free of charge at https://pubs.acs.org/doi/10.1021/acs.joc.3c01927.

^{1}H, ^{13}C, and ^{31}P NMR spectral data and photophysical data for all new molecules, X-ray crystallographic data for **8**, cell images of **1** and **8**. (PDF)

Accession Codes

CCDC 2250708 contains the supplementary crystallographic data for this paper. These data can be obtained free of charge via www.ccdc.cam.ac.uk/data_request/cif, or by emailing data_request@ccdc.cam.ac.uk, or by contacting The Cambridge Crystallographic Data Centre, 12 Union Road, Cambridge CB2 1EZ, UK; fax: +44 1223 336033.

■ AUTHOR INFORMATION

Corresponding Authors

Darren W. Johnson − *Department of Chemistry & Biochemistry and the Materials Science Institute, University of Oregon, Eugene, Oregon 97403-1253, United States;* orcid.org/0000-0001-5967-5115; Email: dwj@uoregon.edu

Michael D. Pluth − *Department of Chemistry & Biochemistry and the Materials Science Institute, University of Oregon, Eugene, Oregon 97403-1253, United States;* orcid.org/0000-0003-3604-653X; Email: pluth@uoregon.edu

Michael M. Haley − *Department of Chemistry & Biochemistry and the Materials Science Institute, University of Oregon, Eugene, Oregon 97403-1253, United States;* orcid.org/0000-0002-7027-4141; Email: haley@uoregon.edu

Authors

Jeremy P. Bard − *Department of Chemistry & Biochemistry and the Materials Science Institute, University of Oregon, Eugene, Oregon 97403-1253, United States; Department of Chemistry, Washington College, Chestertown, Maryland 21620-1438, United States;* orcid.org/0000-0001-6135-0977

Sarah G. Bolton − *Department of Chemistry & Biochemistry and the Materials Science Institute, University of Oregon, Eugene, Oregon 97403-1253, United States*

Holden J. Howard − *Department of Chemistry & Biochemistry and the Materials Science Institute, University of Oregon, Eugene, Oregon 97403-1253, United States*

J. Nolan McNeill − *Department of Chemistry & Biochemistry and the Materials Science Institute, University of Oregon, Eugene, Oregon 97403-1253, United States;* orcid.org/0000-0002-8401-2388

Thaís P. de Faria − *Department of Chemistry & Biochemistry and the Materials Science Institute, University of Oregon, Eugene, Oregon 97403-1253, United States*

Lev N. Zakharov − *CAMCOR, University of Oregon, Eugene, Oregon 97403-1433, United States*

Complete contact information is available at: https://pubs.acs.org/10.1021/acs.joc.3c01927

Notes

The authors declare no competing financial interest.

■ ACKNOWLEDGMENTS

We thank the National Science Foundation (CHE-1607214 and CHE-2107425) for support of this research. We are grateful to Joshua E. Barker for obtaining the HRMS via a CAMCOR facility supported by the NSF (CHE-1625529). This work was also supported by the Bradshaw and Holzapfel Research Professorship in Transformational Science and Mathematics to D.W.J.

■ REFERENCES

(1) Lakowicz, J. R. *Principles of Fluorescence Spectroscopy*, 3rd ed.; Springer: New York, 2006.

(2) Waggoner, A. Covalent labeling of proteins and nucleic acids with fluorophores. *Methods Enzymol.* **1995**, *246*, 362−373.

(3) Johnson, I. Fluorescent probes for living cells. *Histochem. J.* **1998**, *30*, 123−140.

(4) Petit, J.-M.; Denis-Gay, M.; Ratinaud, M.-H. Assessment of fluorochromes for cellular structure and function studies by flow cytometry. *Biol. Cell* **1993**, *78*, 1−13.

(5) Johnsson, N.; Johnsson, K. Chemical Tools for Biomolecular Imaging. *ACS Chem. Biol.* **2007**, *2*, 31−38.

(6) Goddard, J.-P.; Reymond, J.-L. Enzyme assays for high-throughput screening. *Curr. Opin. Biotechnol.* **2004**, *15*, 314−322.

(7) Giepmans, B. N. G.; Adams, S. R.; Ellisman, M. H.; Tsien, R. Y. The Fluorescent Toolbox for Assessing Protein Location and Function. *Science* **2006**, *312*, 217−224.

(8) Zhang, J.; Campbell, R. E.; Ting, A. Y.; Tsien, R. Y. Creating new fluorescent probes for cell biology. *Nat. Rev. Mol. Cell Biol.* **2002**, *3*, 906−918.

(9) Valeur, B.; Berberan-Santos, M. N. *Molecular Fluorescence: Principles and Applications*, 2nd ed.; Wiley-VCH: Weinheim, Germany, 2012.

(10) Frangioni, J. V. In vivo near-infrared fluorescence imaging. *Curr. Opin. Chem. Biol.* **2003**, *7*, 626−634.
(11) Lavis, L. D.; Schnermann, M. J. Rejuvenating old fluorophores with new chemistry. *Curr. Opin. Chem. Biol.* **2023**, *75*, No. 102335.
(12) Wolfbeis, O. S. The fluorescence of organic natural products. In *Molecular Luminescence Spectroscopy: Methods and Applications*—Part 1; Schulman, S. G., Ed.; Wiley: New York, 1985; pp 167−317.
(13) Sun, W.-C.; Gee, K. R.; Haugland, R. P. Synthesis of novel fluorinated coumarins: Excellent UV-light excitable fluorescent dyes. *Bioorg. Med. Chem. Lett.* **1998**, *8*, 3107−3110.
(14) Hinkeldey, B.; Schmitt, A.; Jung, G. Comparative Photostability Studies of BODIPY and Fluorescein Dyes Using Fluorescence Correlation Spectroscopy. *ChemPhysChem* **2008**, *9*, 2019−2027.
(15) Song, L.; Hennink, E. J.; Young, T.; Tanke, H. J. Photobleaching kinetics of fluorescein in quantitative fluorescence microscopy. *Biophys. J.* **1995**, *68*, 2588−2600.
(16) Sjoback, R.; Nygren, J.; Kubista, M. Absorption and fluorescence properties of fluorescein. *Spectrochim. Acta, Part A* **1995**, *51*, L7−L21.
(17) Song, L.; Varma, C. A.; Verhoeven, J. W.; Tanke, H. Influence of the triplet excited state on the photobleaching kinetics of fluorescein in microscopy. *Biophys. J.* **1996**, *70*, 2959−2968.
(18) Lavis, L. D.; Raines, R. T. Bright Building Blocks for Chemical Biology. *ACS Chem. Biol.* **2014**, *9*, 855−866.
(19) Lavis, L. D.; Raines, R. T. Bright Ideas for Chemical Biology. *ACS Chem. Biol.* **2008**, *3*, 142−155.
(20) Bard, J. P.; Johnson, D. W.; Haley, M. M. Bumpy Roads Lead to Beautiful Places: The Twists and Turns in Developing a New Class of PN-Heterocycles. *Synlett* **2020**, *31*, 1862−1877.
(21) Vonnegut, C. L.; Shonkwiler, A. M.; Khalifa, M. M.; Zakharov, L. N.; Johnson, D. W.; Haley, M. M. Facile Synthesis and Properties of 2-λ^5-Phosphaquinolines and 2-λ^5-Phosphaquinolin-2-ones. *Angew. Chem., Int. Ed.* **2015**, *54*, 13318−13322.
(22) McNeill, J. N.; Karas, L. J.; Bard, J. P.; Fabrizio, K.; Zakharov, L. N.; MacMillan, S. N.; Brozek, C. K.; Wu, J. I.; Johnson, D. W.; Haley, M. M. Controlling Tautomerization in Pyridine-Fused Phosphorus-Nitrogen Heterocycles. *Chem.—Eur. J.* **2022**, *28*, No. e202200472.
(23) Bard, J. P.; McNeill, J. N.; Zakharov, L. N.; Johnson, D. W.; Haley, M. M. Thionation of the 2-λ^5-Phosphaquinolin-2-one Scaffold with Lawesson's Reagent. *Isr. J. Chem.* **2021**, *61*, 217−221.
(24) Bard, J. P.; Deng, C.-L.; Richardson, H. C.; Odulio, J. M.; Barker, J. E.; Zakharov, L. N.; Cheong, P. H.-Y.; Johnson, D. W.; Haley, M. M. Synthesis, Photophysical, and Dimerization Properties of 2-λ^5-Phosphaquinolin-2-ones. *Org. Chem. Front.* **2019**, *6*, 1257−1265.
(25) Bard, J. P.; Bates, H. J.; Deng, C.-L.; Zakharov, L. N.; Johnson, D. W.; Haley, M. M. Amplification of the Quantum Yields of 2-λ^5-Phosphaquinolin-2-ones Through Phosphorus Center Modification. *J. Org. Chem.* **2020**, *85*, 85−91.
(26) Lipinski, C. A.; Lombardo, F.; Dominy, B. W.; Feeney, P. J. Experimental and computational approaches to estimate solubility and permeability in drug discovery and development settings. *Adv. Drug Delivery Rev.* **1997**, *23*, 3−25.
(27) Daina, A.; Michielin, O.; Zoete, V. SwissADME: a free web tool to evaluate pharmacokinetics, drug-likeness and medicinal chemistry friendliness of small molecules. *Sci. Rep.* **2017**, *7*, 42717.
(28) Carroll, C. N.; Berryman, O. B.; Johnson, C. A.; Zakharov, L. N.; Haley, M. M.; Johnson, D. W. Protonation activates anion binding and alters binding selectivity in new inherently fluorescent 2,6-bis(2-anilinoethynyl)pyridine bisureas. *Chem. Commun.* **2009**, 2520−2522.
(29) Kourounakis, A. P.; Xanthopoulos, D.; Tzara, A. Morpholine as a privileged structure: A review on the medicinal chemistry and pharmacological activity of morpholine containing bioactive molecules. *Med. Res. Rev.* **2020**, *40*, 709−752.
(30) Hoang, D. Q.; Borisova, E. Y.; Borisova, N. Y.; Asilova, N. Y.; Kaldryrkaeva, O. S.; Arzamastsev, E. V.; Terekhova, O. A.; Afanaseva, E. Y.; Levitskaya, E. L. Synthesis and biological activity of arylaliphatic *N*-(2-aminoethyl)-*N*-(2-hydroxy-2-phenylethyl)carboxamides. *Russ. Chem. Bull.* **2018**, *67*, 131−136.
(31) Dunn, K. W.; Kamocka, M. M.; McDonald, J. H. A practical guide to evaluating colocalization in biological microscopy. *Am. J. Physiol. Cell Physiol.* **2011**, *300*, C723−C742.
(32) Brouwer, A. M. Standards for photoluminescence quantum yield measurements in solution. *Pure Appl. Chem.* **2011**, *83*, 2213−2228.

https://doi.org/10.1021/acs.joc.3c01927
J. Org. Chem. XXXX, XXX, XXX−XXX